# Valence states of copper ions and electronic structure of $LiCu_2O_2$

D. A. Zatsepin, V. R. Galakhov, M. A. Korotin, V. V. Fedorenko, and E. Z. Kurmaev
*Institute of Metal Physics, Russian Academy of Sciences-Ural Division, 620219 Yekaterinburg GSP-170, Russia*

S. Bartkowski and M. Neumann
*Universität Osnabrück, Fachbereich Physik, D-49069 Osnabrück, Germany*

R. Berger
*Institute of Chemistry, Ångström Laboratory, Uppsala University, Box 538, S-751 21 Uppsala, Sweden*
(Received 16 June 1997)

The electronic structure of $LiCu_2O_2$ was studied using x-ray emission (Cu $L_\alpha$, O $K_\alpha$) and photoelectron spectroscopy (valence band and core levels) as well as band-structure calculations in terms of local spin-density approximation (LSDA) and LSDA+$U$ approaches. According to the x-ray-emission and photoelectron spectra the valence states of the Cu atoms are found to be mixed, i.e., 2+ and 1+. The LSDA calculations are contradictory to the experimental data and cannot reproduce the band gap and magnetic properties of $LiCu_2O_2$. The LSDA+$U$ calculations describe the insulator and antiferromagnetic properties much better but the overestimation of the screened Coulomb parameter $U$ leads to a binding-energy shift of the $Cu^{II}$ $3d$ states and this distorts the proper modeling of the valence-band structure. The magnetic structure of $LiCu_2O_2$ is discussed, taking our LSDA+$U$ band-structure calculations into account. [S0163-1829(98)04108-3]

## I. INTRODUCTION

$LiCu_2O_2$ is a compound with mixed-valence copper synthesized recently.[1,2] It was found that $LiCu_2O_2$ is orthorhombic, described by the space group *Pnma* (62) with the unit-cell parameters $a=5.72$ Å, $b=2.86$ Å, and $c=12.41$ Å within a certain homogeneity range.[3,4] The structure was described in Ref. 3 and contains equal amounts of $Cu^I$ and $Cu^{II}$ atoms, ordered on distinct crystallographic sites. An analogous sodium oxocuprate has also been characterized.[5] The $Cu^I$ atoms coordinate two oxygen atoms whereas the $Cu^{II}$ atoms have 4+1 neighbors. $Cu^{II}$ has basically a square environment, and $CuO_4$ units are connected by chains as in CuO. However, two chains run parallel and are connected in such a way that a fifth (apex) oxygen atom is shared with the adjacent chain. These double chains are connected by $LiO_5$ double chains where Li has more even distances, i.e., in contrast to the $Cu^{II}$ atoms the Li lies centered within its $O_5$ pyramid. Thus, alternating double parallel chains, containing either Li or Cu atoms, form the sheets which are interconnected by $Cu^I$ in O-Cu-O pillars.

$LiCu_2O_2$ is an antiferromagnetic insulator with a Néel temperature of 40 K above which the susceptibility obeys the Curie-Weiss law with $\mu_{\text{eff}}=1.93\ \mu_B$/formula unit.[1] The type of the magnetic arrangement of the copper atoms was not established, and the electronic structure of $LiCu_2O_2$ was also unknown up to now.

In this paper, a study of the electronic structure of $LiCu_2O_2$ is presented that includes *ab initio* band-structure calculations in terms of LSDA and LSDA+$U$ approaches together with x-ray emission (Cu $L_\alpha$, O $K_\alpha$) and photoelectron (valence band and core levels) measurements. The two local magnetic structures of $LiCu_2O_2$ are discussed in comparison to the band-structure calculations.

## II. EXPERIMENTAL AND COMPUTATIONAL DETAILS

### A. Sample preparation and experimental details

$LiCu_2O_2$ was prepared by heating mixtures of CuO and $Li_2CO_3$ according to the appropriate stoichiometry, ground together and compacted. The two compounds react with each other at temperatures above 900 °C.[2] X-ray powder diffraction phase analysis was used for the identification of the products. In early stages, before full homogeneity was achieved, other phases such as $LiCu_3O_3$ and $Li_2CuO_2$ were present. A final heat treatment at 960 °C gave a single-phase specimen except for traces of $Li_2CuO_2$, which were completely removed by treating the powder with aqueous ammonia in which it decomposes into soluble products.

The cell parameters were determined using a Guinier-Hägg focusing camera with strictly monochromatic Cu $K_{\alpha_1}$ radiation. Silicon was used as an internal standard ($a=5.431065$ Å at 25 °C). The resulting cell parameters of $LiCu_2O_2$ were $a=5.7260(4)$ Å, $b=2.8587(2)$ Å, and $c=12.4137(7)$ Å.[4]

The x-ray photoelectron spectra (XPS) were measured with a PHI 5600 ci Multitechnique System using monochromatic Al $K_\alpha$ radiation. The sintered specimen of $LiCu_2O_2$ was investigated after breaking it in vacuum. An Au foil was used for calibrating the spectra, taking $E_B(\text{Au } 4f_{7/2})=84.0$ eV as a reference. The representative energy resolution of approximately 0.4 eV was determined at the Fermi level of the Au foil.

The Cu $L_\alpha$ and O $K_\alpha$ emission spectra (XES) were obtained with a JCXA-733 electron-probe microanalyzer, operating the x-ray tube at 5 kV and 100 nA. We used the $L_\alpha$ spectrum of pure Cu (929.7 eV) and O $K_\alpha$ spectrum of MgO (525.4 eV) for calibrating the instrument. The instrumental broadening of the Cu $L_\alpha$ and O $K_\alpha$ spectra was about 0.8 eV and 0.5 eV, respectively.

 © 1998 The American Physical Society

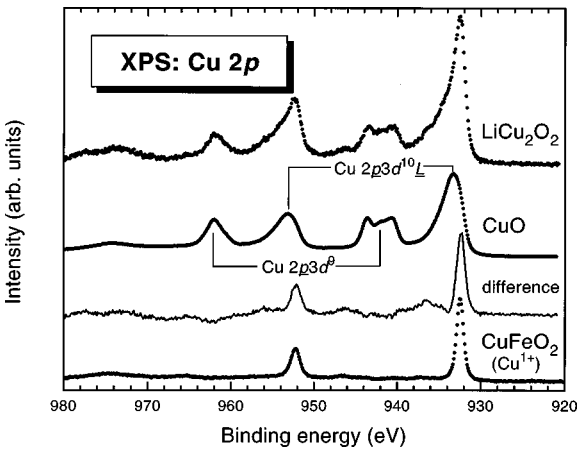


FIG. 1. XPS Cu 2*p* spectra of $LiCu_2O_2$, CuO and their difference in comparison with the Cu 2*p* spectrum of $CuFeO_2$. The first two spectra are normalized to the intensity of satellite.

### B. Computational details

We used two approaches for investigating the electronic structure of $LiCu_2O_2$. The first one is conventional LSDA (local-spin-density approximation) using the linear muffin-tin orbital (LMTO) method in the atomic sphere approach, and the second one is the basis-set independent LSDA+$U$ approach[6] using the same LMTO method. The second approach includes correlation effects in the calculation scheme. The values of radii (in a.u.) were chosen as $r(\mathrm{Cu})=2.7$, $r(\mathrm{O})=2.2$, $r(\mathrm{Li})=2.198$. Four empty spheres (es's) per unit cell were introduced with $r(\mathrm{es})=2.2$ a.u. to simulate $Cu^{I}$-es planes. For the Cu atoms, the parameters for the screened Coulomb potential $U$ and exchange potential $J$ were found to be $U=7.87$ eV, $J=0.9$ eV. The tetrahedron method was used with 36 **k** points for the integration over the Brillouin zone during the course of the self-consistency. All calculations were performed for the triclinic Bravais lattice without inversion to allow the system to choose an appropriate spin order by itself during the self-consistency loops.

## III. RESULTS AND DISCUSSION

### A. X-ray photoelectron core-level spectra

Figure 1 shows the Cu 2*p* x-ray photoelectron spectrum of $LiCu_2O_2$ in comparison with those of CuO (Ref. 7) and $CuFeO_2$.[8] The difference between the XPS $LiCu_2O_2$ and CuO spectra, normalized to the intensity of the satellite, is also given.

The XPS CuO spectrum exhibits the main lines at 933.3 eV and 953.2 eV and intense satellites on the high-binding-energy side (939–945 eV and 959–964 eV). The XPS spectrum of $LiCu_2O_2$ is characterized by similar spectral features. However, one can see a substantial energy shift of the main lines to lower binding energies (932.5 eV and 952.4 eV, respectively) and these bands are significantly narrower. As for CuO a shoulder clearly manifests itself within the energy range from 933–939 eV, near the main line. Additionally, both satellite energy positions coincide with those of CuO, but their intensity ratio $I_s/I_m$ is smaller by a factor of about 2 (here $I_s$ denotes the satellite intensity and $I_m$ the intensity of the corresponding $2p_{3/2}$ main line).

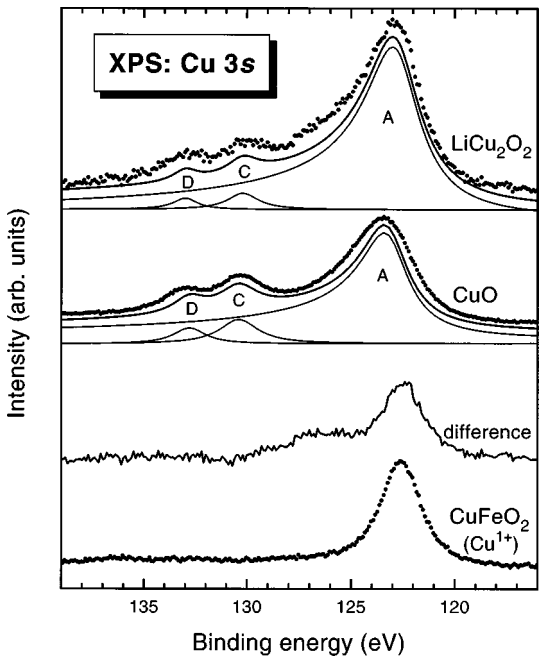


FIG. 2. XPS Cu 3*s* spectra of $LiCu_2O_2$, CuO and their difference in comparison with the Cu 3*s* spectra of $CuFeO_2$. The first two spectra are normalized to the intensity of the satellite.

The XPS Cu 2*p* spectra were interpreted within the simple *charge-transfer* model described by van der Laan *et al.*[9] and Zaanen, Westra, and Sawatzky.[10] In their approach, the main peaks correspond to $2p^5 3d^{10}\underline{L}$ final states, whereas the satellite structures correspond to $\overline{2}p^5 3d^9$ final states (here $\underline{L}$ denotes a hole on the ligand after the so-called charge-transfer processes).

Since $Cu^{1+}$ compounds exhibit XPS Cu 2*p* spectra with distinctly smaller binding energies than $Cu^{2+}$ compounds,[11] the energy shifts of the XPS main lines of $LiCu_2O_2$ can reflect the presence of $Cu^{1+}$ valence states in this oxide. The positions of the XPS Cu 2*p* main lines of $CuFeO_2$ (932.4 eV and 952.2 eV, respectively) agree well with those of $LiCu_2O_2$. In $CuFeO_2$ the Cu atoms are also in the valence state 1+.[8] Thus, coexistence of $Cu^{1+}$ ($Cu^{I}$) and $Cu^{2+}$ ($Cu^{II}$) ions in $LiCu_2O_2$ can be concluded, and is strongly supported by the difference spectrum shown in Fig. 1. A spectral feature seen at about 935 eV in the XPS $LiCu_2O_2$ and the difference spectrum is apparently caused by $Cu(OH)_2$ impurities.[11] These were not noticed in x-ray diffraction and were probably created in the final washing step.

The XPS Cu 3*s* core-level spectra of the investigated oxides are given in Fig. 2. The exchange splitting of $Cu^{II}$ $3s^1 3d^9$ states (features *C* and *D*) can be seen, whereas the feature *A* is not split because it originates from the $3d^{10}$ states, namely, the $Cu^{I}$ $3s^1 3d^{10}$ and $Cu^{II}$ $3s^1 3d^{10}\underline{L}$ states. The magnitude of the *C*-*D* splitting is determined by the expression

$$\Delta E_{3s}=\frac{2S+1}{5}G^2(3s,3d),$$

where $S$ is the local $3d$ spin in the ground state and $G^2(3s,3d)$ is the Slater exchange integral between $3s$ and $3d$ electrons. The meaning of $\Delta E_{3s}$ is approximately the

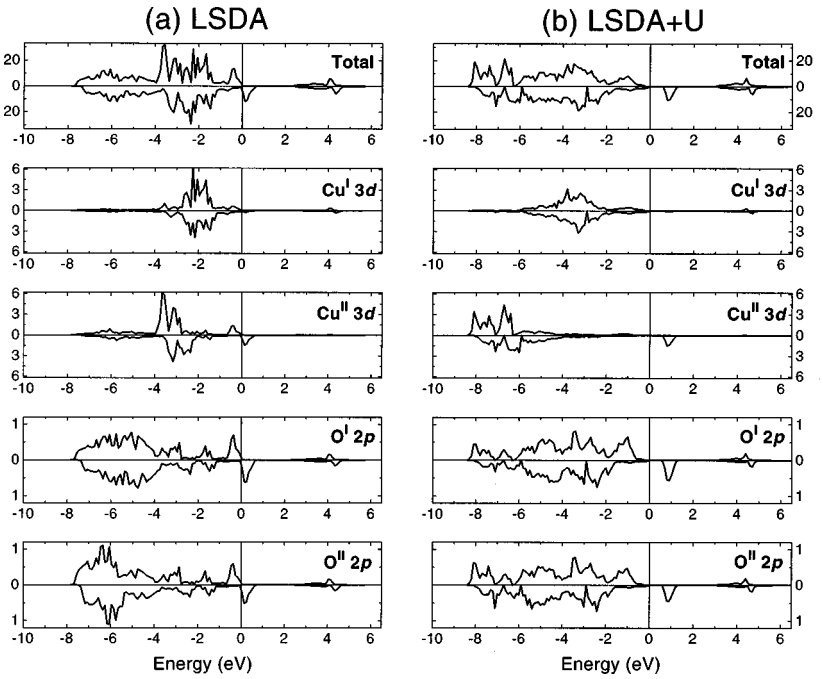


FIG. 3. (a) Densities of states calculated using the LSDA approximation; (b) densities of states calculated using the LSDA+$U$ approximation. The partial DOS is given in states/(eV spin atom) and the total one is given in states/(eV spin cell). $O^{I}$ and $O^{II}$ denote oxygen atoms at different crystallographic sites.[3,4]

same in both CuO and $LiCu_2O_2$ and is about 2.6 eV. As before we have obtained the difference spectrum in Fig. 2 and compared it with the Cu 3$s$ spectrum of $CuFeO_2$. The shoulder seen in the difference spectrum at about 126 eV is probably connected with the presence of $Cu(OH)_2$ impurities as discussed before.

As a matter of fact, all the reported results prove the presence of both $Cu^{1+}$ and $Cu^{2+}$ ions in $LiCu_2O_2$.

### B. Band-structure calculations

Although the type of the magnetic arrangement of the Cu atoms in $LiCu_2O_2$ is unknown, one may assume that copper atoms forming the $Cu^{I}O_2$ dumbbells are nonmagnetic (this is confirmed by further calculations), and that only the $Cu^{II}$ atoms, forming double sheets of chains of $Cu^{II}O_4$ squares, carry the magnetic moments. Based on this assumption it is possible to consider the two simplest types of magnetic structure: first, an antiferromagnetic arrangement of the sheets with parallel spins on the $Cu^{II}$ atoms within every sheet, and second, an antiferromagnetic arrangement of magnetic moments within the sheets. Both types of magnetic structure were checked in the present work.

The LSDA densities of states (DOS) for ferromagnetic $LiCu_2O_2$ exhibit a ''half-metal'' character in the energy spectrum: the majority spin density is located just below the Fermi level whereas the minority spin density is crossed by the Fermi level [see Fig. 3(a)]. The states in the energy range from $-8$ to $-4$ eV are mainly formed by oxygen 2$p$ states. The Cu $d$ states are found in the energy range from $-4$ to $-1$ eV. A strong mixture of $p$ and $d$ states occurs $\pm 1$ eV around the Fermi level. The DOS at about 4 eV above the Fermi level is an admixture of Cu $d$ and O $p$ states to the states of Li and es.

An unexpected result was obtained with respect to the magnetic order in this compound. Independent of the initial spin arrangement of the $Cu^{II}$ atoms (see discussion above), the final spin order after a self-consistency course was ferromagnetic. The value of the $Cu^{I}$ spin moment appears to be negligibly small. Simultaneously, an essential polarization of the oxygen $p$ states occurs: the value of the spin magnetic moment on the oxygen $p$ shell is only two times smaller than that of the $d$ shell of $Cu^{II}$.

The LSDA+$U$ approach led to another picture of the energy bands of ferromagnetic $LiCu_2O_2$ [Fig. 3(b)]. Here, an insulator with an energy gap of 0.66 eV was obtained. This energy gap is opened between mainly oxygen $p$ states on the low-energy side and hybridized $d$-$p$ states of $Cu^{II}$ and oxygen. Now the DOS in the low-energy range is formed by $Cu^{II}$ $d$ states with an admixture of $p$ states. The DOS of $Cu^{II}$ exhibits sharp bands split into lower and upper Hubbard bands (in the model Hamiltonian approach) whereas the $Cu^{I}$ DOS does not form a wide band. The DOS of oxygen is distributed rather uniformly along the whole energy interval. The values of the calculated magnetic moments (all values in $\mu_B$) are 0.01 for $Cu^{I}$, 0.53 for $Cu^{II}$, 0.25 for $O^{I}$, 0.20 for $O^{II}$, 0.01 for Li, and $-0.01$ for es atoms.

The spin magnetic moment per formula unit is found to be 1.0 $\mu_B$. In the paramagnetic regime, this value corresponds to $\mu_{eff}=1.73$ $\mu_B$ [in the ''spin-only'' approximation, often valid for 3$d$ metals, $\mu_{eff}=2\sqrt{S(S+1)}$, where $S$ is a total spin] and is comparable with the experimental value of 1.93 $\mu_B$ evaluated from the high-temperature part of the magnetic susceptibility curve.[1] Taking the results of the calculations and common copper crystal chemistry into account, one can associate the copper atoms in the dumbbells with $Cu^{1+}$ ions (formal configuration $d^{10}$) and the state of the copper atoms in squares with $Cu^{2+}$ ions (formal configuration $d^9$).

### C. Valence-band spectra

XPS valence-band spectra provide information about the total DOS distribution when also considering the cross sections of states, whereas XES Cu $L_\alpha$ and O $K_\alpha$ spectra reflect the contributions of the partial densities of the occupied Cu 3$d$ and O 2$p$ states, respectively.

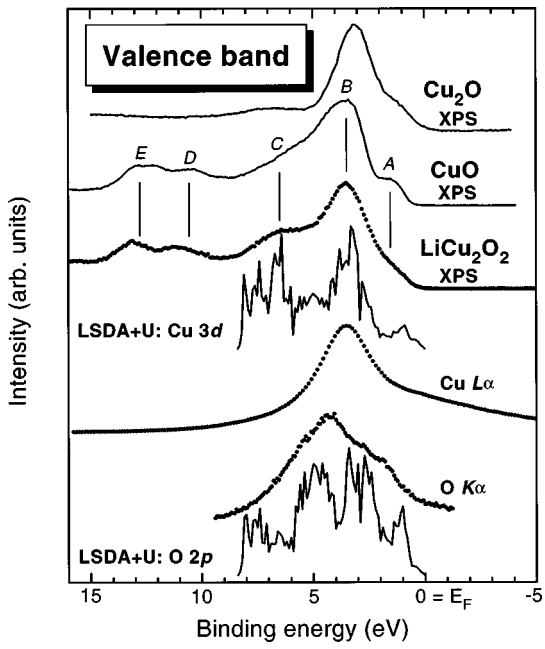


FIG. 4. The XPS valence band and Cu $L_\alpha$, O $K_\alpha$ x-ray emission spectra of $LiCu_2O_2$. The XPS valence-band spectra of $Cu_2O$ (taken from Ref. 13) and CuO are added for comparison. The XES spectra were brought to a common energy scale using the binding energies of core levels.

The XPS valence-band as well as the XES Cu $L_\alpha$ ($3d4s \rightarrow 2p_{3/2}$ electron transition) and O $K_\alpha$ ($2p \rightarrow 1s$ electron transition) spectra of $LiCu_2O_2$ are given in Fig. 4. The latter were brought to the scale of binding energies with respect to the Fermi level using the respective XPS core-level binding energies [$E_B$(Cu $2p_{3/2}$) = 932.5 ± 0.1 eV and $E_B$(O $1s$) = 530.1 ± 0.1 eV].

The XPS valence-band spectrum of $LiCu_2O_2$ contains five main features labeled $A-E$: the shoulder $A$ at 1 eV, the main line $B$ at 3.5 eV, the shoulder $C$ at 6 eV, and the satellite bands $D$ and $E$ with the maxima at about 11 eV and 13 eV. The ratio of cross sections $\sigma$(Cu $3d$):$\sigma$(O $2p$) equals 1:0.02 for Al $K_\alpha$ excitation.[12] This means that the XPS spectrum results mainly from Cu $3d$ states. While the satellite band is due to $Cu^{II}$ $d^8$ final states,[13] it remains to discuss the origin of the XPS main line and the shoulders.

The coincidence of the XPS main peak with the Cu $L_\alpha$ x-ray emission band also proves the Cu $3d$ character of the XPS spectrum. However, the XES Cu $L_\alpha$ is narrower than the Cu $3d$ states in the XPS valence-band spectra. Such a discrepancy can be associated with differences in the transition probabilities from the top and the bottom part of the valence band ($3d4s \rightarrow 2p_{3/2}$ electron transition). For example, it is well known that in the Fe $L_\alpha$ x-ray emission band, the transition from the top part of the valence band has a higher probability than that from the bottom part by a factor of 1.8.[14,15] This results in a decrease of the bottom band intensity at the bottom of the valence band, which then appears to be narrower.

According to the LSDA+$U$ calculations the shoulder $C$ at 6 eV can be associated mainly with the $Cu^{II}$ $3d$ states whereas the main line $B$ corresponds mainly to $Cu^{I}$ $3d$ states [Fig. 3(b) and Fig. 4]. The XPS valence-band spectrum of CuO (features $A,B,C$ in the binding-energy range from 0 to 7 eV) is related to the $3d^9\underline{L}$ final states.[13] The features $A,B,C$ are of singlet $^1A_1$, triplet $^3B_1$, and triplet $^3A_1$ symmetries, respectively. Next, one can see a coincidence of the shape and energy position of the satellites $D$ and $E$ in the XPS spectra of both CuO and $LiCu_2O_2$. This means that the Coulomb interaction energy $U$ and the charge transfer parameter $\Delta$ for $LiCu_2O_2$ are equal to those of CuO. Therefore, the $3d^9\underline{L}$ final states of $LiCu_2O_2$ must be located at the same energy region as for CuO. Conceptually this is not so (Fig. 4).

From the aforesaid it might be assumed that the calculated data are at variance with the experimental ones. Thus we can interpret the latter on the basis of the CuO and $Cu_2O$ XPS valence-band spectra. In terms of such an approach, the shoulder $A$ at 1 eV is of singlet $A_{1g}$ character (antibonding states) while the origin of the main line $B$ is associated with the partial contributions of $Cu^{II}$ $3d$ and $Cu^{I}$ $3d$ states. Such a conclusion was made after a closer inspection of the experimental data.

As for the calculated O $2p$ states there is a good coincidence with the XES O $K_\alpha$ spectrum (see Fig. 4). In this case, the shoulder at 1 eV reflects the admixture of antibonding $p$-$d$ states while the region from 4 eV up to 10 eV belongs to the bonding ones.

Therefore, we can say with reasonable confidence that the LSDA+$U$ calculations interpret the occupied Cu $3d$ and O $2p$ states correctly, but the overestimation of the screened Coulomb parameter $U$ results in a binding energy shift of $Cu^{II}$ $3d$ states and this distorts the modeling of the valence band structure.

## IV. CONCLUSIONS

Taking all the aforesaid into consideration the following conclusions were made: (i) The valency state of $Cu^{I}$ atoms in dumbbells is associated with $Cu^{1+}$ ions (formal configuration $d^{10}$) and that of $Cu^{II}$ atoms in squares with $Cu^{2+}$ ions (formal configuration $d^9$). This idea agrees well with the XPS (core level, valence band) and XES (Cu $L_\alpha$, O $K_\alpha$) experimental data as well as with the experience from the copper-oxygen crystal chemistry. (ii) The results of LSDA calculations cannot reproduce the electric and magnetic properties (the band gap and magnetic moments). The latter are much better described by LSDA+$U$ calculations. (iii) The structure of the valence band was studied by XPS and XES. It was established that there is a hybridization of Cu $3d$ and O $2p$ states. (iv) The $Cu^{I}$ $3d$ and O $2p$ states are correctly reproduced by LSDA+$U$ calculations. However, the overestimation of screened Coulomb parameter $U$ leads to the binding-energy shift of the $Cu^{II}$ $3d$ states.

## ACKNOWLEDGMENTS

Financial support from NATO (Grant No. HTECH.LG940861), Deutsche Forschungsgemeinschaft (DFG), the International Project ''Electron Structure of Oxides,'' and the Russian Foundation for Fundamental Research (Grant No. 96-03-32092) are gratefully acknowledged.

[1] S. J. Hibble, J. Köhler, and A. Simon, J. Solid State Chem. **88**, 534 (1990).
[2] R. Berger, J. Less-Common Met. **169**, 33 (1991).
[3] R. Berger, A. Meetsma, and S. van Smaalen, J. Less-Common Met. **175**, 119 (1991).
[4] R. Berger, P. Önnerud, and R. Tellgren, J. Alloys Compd. **184**, 315 (1992).
[5] G. Tams and Hk. Müller-Buschbaum, J. Alloys Compd. **189**, 241 (1992).
[6] A. I. Liechtenstein, V. I. Anisimov, and J. Zaanen, Phys. Rev. B **52**, R5467 (1995).
[7] The CuO single crystal was prepared in the Laboratory of Prof. A. A. Samokhvalov (Institute of Metal Physics, Ural Division of Russian Academy of Sciences, Yekaterinburg).
[8] V. R. Galakhov, A. I. Poteryaev, E. Z. Kurmaev, V. I. Anisimov, St. Bartkowski, M. Neumann, Z. W. Lu, B. M. Klein, and Tong-Rong Zhao, Phys. Rev. B **56**, 4584 (1997).
[9] G. van der Laan, C. Westra, C. Haas, and G. A. Sawatzky, Phys. Rev. B **23**, 4369 (1981).
[10] J. Zaanen, C. Westra, and G. A. Sawatzky, Phys. Rev. B **33**, 8060 (1986).
[11] *Handbook of X-ray Photoelectron Spectroscopy*, edited by J. Chastman (Perkin-Elmer Corp., Phys. Electron. Div., Eden Prairie, MN, 1992).
[12] J. J. Yeh and I. Lindau, At. Data Nucl. Data Tables **32**, 1 (1985).
[13] L. H. Tjeng, Ph.D. thesis, University of Groningen, 1990.
[14] J. H. Wood, Phys. Rev. **117**, 714 (1960).
[15] B. B. Nemoshkalenko, *X-ray Emission Spectroscopy of Metals and Alloys* (Naukova Dumka, Kiev, 1972) (in Russian).